LU TP 17-18
May 2017

STUDY OF THE ELECTRON ELECTRIC DIPOLE MOMENT IN A FROGGATT NIELSEN TWO-HIGGS DOUBLET MODEL

Johannes Sandberg

Department of Astronomy and Theoretical Physics, Lund University

Bachelor thesis supervised by Johan Rathsman

LUND
UNIVERSITY

Abstract

We consider a two Higgs doublet model with a $U(1)$ Froggatt Nielsen mechanism. The Froggatt Nielsen charges of the fermions are chosen such that the correct mass structure and quark mixing matrix is obtained, and such that Flavor Changing Neutral Currents are within experimental limits. We do not assume any discrete symmetry of the lagrangian, and let Charge Parity be violated, both in the Higgs sector, and the Yukawa sector.

In this framework we study the contributions to the electric dipole moment of the electron, originating from Barr-Zee diagrams with a top or bottom quark loop, and neutral Higgs exchange. We use numerical calculations to examine how the dipole moment depends on the mixing angles of the scalars, the complex phases of the Yukawa couplings, and on the masses of the neutral scalars.

We present the results of these calculations for some interesting parameter values. We find that by allowing both Charge Parity violating Higgs mixing, and complex Yukawa couplings, we can get these contributions to cancel out. We also find that, for some reason, the contribution from the top quark is suppressed.

Populärvetenskaplig sammanfattning

Mikrokosmos. En underlig plats styrd av kvantmekanikens märkliga lagar, och där all vår vardagliga intuition raskt kastas ut genom fönstret. Under 1900-talet har vår förståelse av denna främmande värld ökat något enormt, vilket mot senare halvan av århundradet kulminerade i formuleringen av den så kallade standardmodellen. Standardmodellen är den vetenskapliga teori som utgör grunden för vår förståelse av de minsta byggstenarna i vår värld, elementarpartiklarna, och den beskriver allt ifrån radioaktivt sönderfall, till hur atomer hålls samman, till varför magneter dras till varandra.

Trots dess enorma framgång i att förklara hur universum fungerar, så vet vi dock även att den inte är hela pusslet, och det finns många saker som standardmodellen inte förklarar. Detta innebär att man måste undersöka nya idéer, som utökar standardmodellen på olika sätt. I detta arbete undersöks en sådan utökning. I standardmodellen får saker och ting massa, bland annat tack vare det så kallade Higgs-fältet. Detta Higgs-fält kan liknas vid en tjock sirap, som då partiklarna måste vada genom, vilket gör att de verkar mer massiva. Existensen av detta Higgs-fält bekräftades genom upptäckten av Higgs-bosonen, vilket ledde till nobelpriset i fysik år 2013.

I detta arbete studeras vad som händer ifall man har *två* stycken Higgs-fält, i stället för bara ett; det visar sig nämligen att det inte finns något som direkt hindrar att det skulle kunna finnas fler än ett Higgs-fält. Man har dessutom undersökt en annan spekulativ modell, som skulle kunna förklara varför elementarpartiklarna har så olika massor, jämfört med varandra. Tillsammans bidrar dessa två tillägg till att elektronen får ett så kallat elektriskt dipolmoment. Detta innebär att elektronens laddning blir aningen ojämt fördelad, och hur dipolmomentet påverkas av de två tidigare nämnda tilläggen är det som studeras i detta arbete.

Contents

Abbreviations

2HDM	Two Higgs Doublet Model
FCNC	Flavor Changing Neutral Currents
VEV	Vacuum Expectation Value
FN	Froggatt Nielsen
BSM	Beyond Standard Model
EDM	Electric Dipole Moment
eEDM	Electron Electric Dipole Moment
SM	Standard Model

Acknowledgments

I would like to thank J. Rathsman for supervising this thesis, E. Andersson for providing me with the Froggatt Nielsen charges, and N. Hermansson Truedsson for letting me use his modified code, and for helping me implement it.

1 Introduction

In the standard model, electroweak symmetry is broken by the scalar Higgs field obtaining a non-zero vacuum expectation value [1]. This gives mass to the weak bosons, with their masses being given by the parameters of the Higgs potential. The fermions, disregarding neutrinos, are also given mass, by letting them couple to the Higgs field. This, however, does not explain why the fermions have the masses they do, since this is determined by the couplings to the Higgs field, which are free parameters. If these couplings, and thus the fermion masses, are free parameters, then one could ask why the fermion masses cover such a large range. For instance, the top quark is $\sim 10^5$ times heavier than the up quark [2]. One attempt to explain this orders of magnitude large difference was presented by C. D. Froggatt and H. B. Nielsen [3]. In the Froggatt Nielsen mechanism the fermion mass hierarchy is explained by having the fermions couple to the Higgs field indirectly, going through a chain of heavy, beyond standard model, particles. This mechanism also gives an explanation to why the Cabibbo Kobayashi Maskawa (CKM) quark mixing matrix is the way it is.

The Froggatt Nielsen mechanism works, not only in the standard model Higgs mechanism, but also in the two Higgs Doublet Model (2HDM). This is useful, since many beyond standard model frameworks, such as supersymmetry, require at least two Higgs doublets [4]. There are, however, other reasons to study the 2HDM, in itself. To begin with, the 2HDM is a simple extension to the standard model, providing predictions that can potentially be tested at currently obtainable energy scales. Furthermore, the 2HDM provides a new source of Charge Parity (CP) violation, which is a requirement of electroweak baryogenesis [5]. The Froggatt Nielsen mechanism has recently been studied in a two Higgs doublet framework, see [6].

One potential problem with two Higgs doublet models is that they give rise to tree level Flavor Changing Neutral Currents (FCNC). There are many ways to remove such FCNC, such as imposing a discrete symmetry on the lagrangian, or requiring that the couplings to the different scalar fields be proportional to each other [7]. One consequence of a CP-violating 2HDM is that there will be additional contributions to the Electric Dipole Moment (EDM) of the electron, beyond that of the standard model. This was pointed out by Weinberg [8], and later expanded upon by S. M. Barr and A. Zee [9].

In this study we will let the Yukawa couplings be decided by the Froggatt Nielsen mechanism, with charges assigned such that we get the correct fermion masses, and the correct CKM matrix, while also minimizing FCNCs. We will then examine how the electron EDM depends on the other parameters of the model, including the scalar mixing angles, the complex phases of the Yukawa couplings, and the masses of the Higgs particles. The remainder of this report is divided into six sections. First we will present the general theory, beginning with the 2HDM in section 2, then proceeding with the 2HDM Froggatt Nielsen mechanism in section 3. In section 4 we present the electric dipole moment, as it arises from a 2HDM, and in section 5 we briefly discusses the program used to perform calculations. In section 6 we present the results of our calculations, and section 7 contains some concluding remarks.

2 Two Higgs Doublet Models

2.1 Standard Model Higgs Mechanism

In the standard model Higgs mechanism, we consider a complex scalar field with a potential [1]

$$V_{Higgs}(\phi) = \mu^2 \phi^\dagger \phi + \lambda \left(\phi^\dagger \phi\right)^2 \tag{1}$$

where μ and λ are potential parameters, and the field ϕ is an $SU(2)$ doublet

$$\phi = \frac{1}{\sqrt{2}} \begin{pmatrix} \phi_1 + i\phi_2 \\ \phi_3 + i\phi_4 \end{pmatrix} = \begin{pmatrix} \phi^+ \\ \phi^0 \end{pmatrix} \tag{2}$$

For $\mu^2 < 0$, the potential will have minima at $\phi^\dagger \phi = -\mu/2\lambda = v^2/2$. We proceed with breaking the symmetry of the potential, choosing the vacuum as

$$\phi_0 = \frac{1}{\sqrt{2}} \begin{pmatrix} 0 \\ v \end{pmatrix} \tag{3}$$

where, $v \approx 246\,\text{GeV}$. Furthermore, perturbations around the vacuum will give rise to particles

$$\phi = \frac{1}{\sqrt{2}} \begin{pmatrix} 0 \\ v + h \end{pmatrix} \tag{4}$$

Note that we have only included the physical scalar particle h, as the charged scalar and the pseudoscalar are removed through an appropriate gauge transformation. The fact that the lower component is non-zero in the vacuum means that the weak gauge bosons become massive, with $m_W\,, m_Z \propto v$.

We can also give mass to the fermions of the standard model, using the Yukawa couplings. We use a notation to denote the fermions where L and Q respectively are column matrices in flavor space, with the weak doublets as their elements

$$Q_L = \begin{pmatrix} \begin{pmatrix} u_L \\ d_L \end{pmatrix} \\ \begin{pmatrix} c_L \\ s_L \end{pmatrix} \\ \begin{pmatrix} t_L \\ b_L \end{pmatrix} \end{pmatrix} \qquad\qquad L_L = \begin{pmatrix} \begin{pmatrix} \nu_{eL} \\ e_L \end{pmatrix} \\ \begin{pmatrix} \nu_{\mu L} \\ \mu_L \end{pmatrix} \\ \begin{pmatrix} \nu_{\tau L} \\ \tau_L \end{pmatrix} \end{pmatrix} \tag{5}$$

and we similarly define the flavor space matrices, U, D, and E, as containing the right handed singlets

$$U_R = \begin{pmatrix} u_R \\ c_R \\ t_R \end{pmatrix} \qquad\qquad D_R = \begin{pmatrix} d_R \\ s_R \\ b_R \end{pmatrix} \qquad\qquad E_R = \begin{pmatrix} e_R \\ \mu_R \\ \tau_R \end{pmatrix} \tag{6}$$

Finally, in order to give mass to the up type quarks, we need to introduce the conjugate doublet. If we have a doublet ϕ, then $\tilde{\phi} = -i\sigma_2\phi^*$ is the conjugate doublet of ϕ, with σ_2 being the second Pauli matrix. This conjugate doublet has the property that it will transform in the same way as ϕ, under $SU(2)$ [1].

$$\phi = \begin{pmatrix} \phi_1 \\ \phi_2 \end{pmatrix} \qquad\qquad \tilde{\phi} = \begin{pmatrix} -\phi_2^* \\ \phi_1^* \end{pmatrix} \tag{7}$$

With this notation we can write out the Yukawa lagrangian as

$$\mathcal{L}_y = \overline{Q}_L Y^D \phi D_R + \overline{Q}_L Y^U \tilde{\phi} U_R + \overline{L}_L Y^E \phi E_R + h.c. \tag{8}$$

where $h.c.$ is used to denote the hermitian conjugate of everything before it.

2.2 Two Scalar Doublets

We now look at the case where we have two scalar doublets, instead of just one. The most general potential for two such scalar fields is [7]

$$\begin{aligned} V =& m_{11}^2 \Phi_1^\dagger \Phi_1 + m_{22}^2 \Phi_2^\dagger \Phi_2 - \left(m_{12}^2 \Phi_1^\dagger \Phi_2 + \text{h.c.} \right) + \frac{\lambda_1}{2} \left(\Phi_1^\dagger \Phi_1 \right)^2 & (9) \\ &+ \frac{\lambda_2}{2} \left(\Phi_2^\dagger \Phi_2 \right)^2 + \lambda_3 \Phi_1^\dagger \Phi_1 \Phi_2^\dagger \Phi_2 + \lambda_4 \Phi_1^\dagger \Phi_2 \Phi_2^\dagger \Phi_1 & (10) \\ &+ \left(\frac{\lambda_5}{2} \left(\Phi_1^\dagger \Phi_2 \right)^2 + \left[\lambda_6 \left(\Phi_1^\dagger \Phi_1 \right) + \lambda_7 \left(\Phi_2^\dagger \Phi_2 \right) \right] \left(\Phi_1^\dagger \Phi_2 \right) + \text{h.c.} \right) & (11) \end{aligned}$$

where the parameters $m_{11,22}^2$ and $\lambda_{1,2,3,4}$ are real, whereas m_{12}^2 and $\lambda_{5,6,7}$ can be complex, in the general case.

Analogously to the standard model Higgs mechanism, minimizing this potential gives us, for the vacuum state [4]

$$\Phi_1 = e^{i\xi_1} \frac{1}{\sqrt{2}} \begin{pmatrix} 0 \\ v_1 \end{pmatrix} \qquad\qquad \Phi_2 = e^{i\xi_2} \frac{1}{\sqrt{2}} \begin{pmatrix} 0 \\ v_2 \end{pmatrix} \tag{12}$$

where the two complex phases ξ_i give rise to spontaneous CP violation. We will, however, assume that there is no such spontaneous CP violation, i.e. that $\xi_1 = \xi_2 = 0$. Perturbations around the vacuum gives rise to eight new fields

$$\Phi_1 = \frac{1}{\sqrt{2}} \begin{pmatrix} H_1^+ \\ v_1 + \phi_1 + iA_1^0 \end{pmatrix} \qquad\qquad \Phi_2 = \frac{1}{\sqrt{2}} \begin{pmatrix} H_2^+ \\ v_2 + \phi_2 + iA_2^0 \end{pmatrix} \tag{13}$$

The scalar doublets can be represented in different bases, connected via orthogonal transforms. Introducing the angle β, with $\tan\beta = v_2/v_1$ [7], we can redefine our doublets as

$$H_1 = \cos(\beta)\Phi_1 + \sin(\beta)\Phi_2 \tag{14}$$

$$H_2 = -\sin(\beta)\Phi_1 + \cos(\beta)\Phi_2 \tag{15}$$

In this basis, called the Higgs basis, we find that only one of the doublets will get a vacuum expectation value, $v = \sqrt{v_1^2 + v_2^2}$, which must be equal to that of the standard model. In the Higgs basis, the two doublets become

$$H_1 = \frac{1}{\sqrt{2}} \begin{pmatrix} G^+ \\ v + \tilde{h}_1 + iG^0 \end{pmatrix} \qquad H_2 = \frac{1}{\sqrt{2}} \begin{pmatrix} H^+ \\ \tilde{h}_2 + i\tilde{h}_3 \end{pmatrix} \tag{16}$$

where $G^\pm$ and G^0 are the Goldstone bosons that get eaten by the weak bosons. Indeed, if one writes out the mass matrices for the neutral and the charged scalars, one will find that $G^\pm$ and G^0 are eigenstates with eigenvalues zero [4]. The CP even scalars $\tilde{h}_1$, $\tilde{h}_2$, and the CP odd scalar $\tilde{h}_3$, are, however, not generally mass eigenstates, but will further mix with each other. Their mixing forms a potential source of CP violation, if there is mixing between $\tilde{h}_3$ and the other two.

We define an $SO(3)$ matrix, $\tilde{R}$, which diagonalizes the squared mass matrix of the neutral scalars, thus relating $\tilde{h}_i$ to the mass eigenstates h_i such that $(\tilde{h}_1, \tilde{h}_2, \tilde{h}_3) = (h_1, h_2, h_3)\tilde{R}$. This matrix can be parameterized in the usual way, using three mixing angles, α_1, α_2, and α_3, such that $\tilde{R} = R_{23}(\alpha_3)R_{13}(\alpha_2)R_{12}(\pi/2 - \alpha_1)$, with the rotation matrices $R_{23,13,12}(\varphi)$ defined as

$$R_{23}(\varphi) = \begin{pmatrix} 1 & 0 & 0 \\ 0 & \cos\varphi & \sin\varphi \\ 0 & -\sin\varphi & \cos\varphi \end{pmatrix} \quad R_{13}(\varphi) = \begin{pmatrix} \cos\varphi & 0 & \sin\varphi \\ 0 & 1 & 0 \\ -\sin\varphi & 0 & \cos\varphi \end{pmatrix} \quad R_{12} = \begin{pmatrix} \cos\varphi & \sin\varphi & 0 \\ -\sin\varphi & \cos\varphi & 0 \\ 0 & 0 & 1 \end{pmatrix} \tag{17}$$

We note that for $\alpha_2 = \alpha_3 = 0$, there will be no mixing between CP-odd and CP-even scalars, and thus no CP violation in the scalar sector. The reason we have defined $\tilde{R}$ with $\pi/2 - \alpha_1$, is for compatibility with the program used to do calculations, see section 5. This is, however, not the only relevant mixing matrix for the neutral scalars. $\tilde{R}$ is defined as the matrix which diagonalizes the mass squared matrix in the *Higgs basis*, but we can also define a mixing matrix, $R = R_{23}(\alpha_c)R_{13}(\alpha_b)R_{12}(\alpha)$, which diagonalizes the squared mass matrix of $(\phi_1, \phi_2, \tilde{h}_3)$[1], see [10]. Note, however, that we use α instead of $\alpha + \pi/2$, again this is for compatibility with the program used to perform calculations. It will be useful to be able to relate these two mixing matrices to each other. In particular, we want a relation betweeen the mixing angles that are used to parameterize them.

From the definition of the two mixing matrices, we have

$$\begin{pmatrix} h_1 \\ h_2 \\ h_3 \end{pmatrix} = \tilde{R} \begin{pmatrix} \tilde{h}_1 \\ \tilde{h}_2 \\ \tilde{h}_3 \end{pmatrix} = R \begin{pmatrix} \phi_1 \\ \phi_2 \\ \tilde{h}_3 \end{pmatrix} = R \begin{pmatrix} \cos\beta & -\sin\beta & 0 \\ \sin\beta & \cos\beta & 0 \\ 0 & 0 & 1 \end{pmatrix} \begin{pmatrix} \tilde{h}_1 \\ \tilde{h}_2 \\ \tilde{h}_3 \end{pmatrix} \tag{18}$$

[1]Recall that $\phi_{1,2}$ are the CP-even scalars in the general basis, whereas $\tilde{h}_3$ is the non-goldstone, CP-odd, scalar, in the Higgs basis. This is a reasonable thing to do, since during the rotation to the Higgs basis, the CP-even states do not mix with the CP-odd states.

where the last step follows directly from the definition of the Higgs basis. We see that

$$\tilde{R} = R \begin{pmatrix} \cos\beta & -\sin\beta & 0 \\ \sin\beta & \cos\beta & 0 \\ 0 & 0 & 1 \end{pmatrix} \tag{19}$$

which, when written out, fully, leads to the conclusion that

$$\alpha_3 = \alpha_c \tag{20}$$
$$\alpha_2 = \alpha_b \tag{21}$$
$$\alpha_1 = \beta - \alpha + \frac{\pi}{2} \tag{22}$$

allowing us to relate the mixing matrix in the Higgs basis, with that of [10], as well as [5]. This allows us to write $\tilde{R}$ in terms of $(\beta - \alpha)$, α_b, and α_c, as

$$\tilde{R} = \begin{pmatrix} c_{\beta-\alpha}c_{\alpha_b} & -s_{\beta-\alpha}c_{\alpha_b} & s_{\alpha_b} \\ -c_{\beta-\alpha}s_{\alpha_b}s_{\alpha_c} + s_{\beta-\alpha}c_{\alpha_c} & c_{\beta-\alpha}c_{\alpha_c} + s_{\beta-\alpha}s_{\alpha_b}s_{\alpha_c} & c_{\alpha_b}s_{\alpha_c} \\ -c_{\beta-\alpha}s_{\alpha_b}c_{\alpha_c} - s_{\beta-\alpha}s_{\alpha_c} & s_{\beta-\alpha}s_{\alpha_b}c_{\alpha_c} - c_{\beta-\alpha}s_{\alpha_c} & c_{\alpha_b}c_{\alpha_c} \end{pmatrix} \tag{23}$$

2.3 Neutral Scalar Couplings to Fermions

We now look for the couplings between the physical neutral scalars, h_i, and the fermions. We consider the Yukawa lagrangian, in the general basis

$$\begin{aligned} \mathcal{L}_y = {} & \overline{Q}_L Y_1^D \Phi_1 D_R + \overline{Q} L Y_2^D \Phi_2 D_R + \overline{Q}_L Y_1^U \tilde{\Phi}_1 U_R + \\ & + \overline{Q}_L Y_2^U \tilde{\Phi}_2 U_R + \overline{L}_L Y_1^E \Phi_1 E_R + \overline{L}_L Y_2^E \Phi_2 E_R + h.c. \end{aligned} \tag{24}$$

where we have used the same notation as earlier. We can go over to the Higgs basis, which will change the Yukawa lagrangian into

$$\begin{aligned} \mathcal{L}_y = {} & \overline{Q}_L \kappa_0^D H_1 D_R + \overline{Q}_L \rho_0^D H_2 D_R + \overline{Q}_L \kappa_0^U \tilde{H}_1 U_R + \\ & + \overline{Q}_L \rho_0^U \tilde{H}_2 U_R + \overline{L}_L \kappa_0^E H_1 E_R + \overline{L}_L \rho_0^E H_2 E_R + h.c. \end{aligned} \tag{25}$$

where the new couplings are defined as

$$\kappa_0^F = \cos(\beta) Y_1^F + \sin(\beta) Y_2^F \tag{26}$$
$$\rho_0^F = -\sin(\beta) Y_1^F + \cos(\beta) Y_2^F \tag{27}$$

with $F = U$, D, E. In the general case both of Y_i^F, and hence also κ_0^F and ρ_0^F, can be complex, which is another potential source of CP violation. They are also not generally diagonal, which poses a problem when one wishes to find the masses, since κ_0^F is related to the mass matrix, $M_0^F = v\kappa_0^F$. Before one can obtain the masses one must diagonalize the mass matrix using a biunitary transform, $M_0^F \to M^F = U_L^F M_0^F U_R^{F\dagger}$, where U_L^F and U_R^F

are both unitary matrices [4]. This transformation will also transform κ_0^F and ρ_0^F into κ^F and ρ^F, where κ^F is now diagonal. This will also transform the weak eigenstates, $F_{L,R}$, of the fermions into the mass eigenstates, $\tilde{F}_{L,R} = U_{L,R}^F F_{L,R}$. We will from now on refer to the mass eigenstates as just $F_{L,R}$, rather than $\tilde{F}_{L,R}$. It is also possible to identify the CKM matrix as

$$V_{CKM} = U_L^U U_L^{D\dagger} \tag{28}$$

In general, the diagonalization of κ will not diagonalize ρ, which can remain non-diagonal, and possibly complex. If ρ is non-diagonal, this will give rise to flavor changing neutral currents, FCNC, at the tree level. In order to avoid FCNC, one usually makes further assumptions in order to remove, or at least limit in size, the off diagonal elements of ρ. The discussion of such can be found in [4], [5], and [10]. In this study, we let the couplings be decided by the Froggatt Nielsen mechanism described in section 3.

We will now write out the Yukawa lagrangian for the down quarks in terms of the scalars $\tilde{h}_i$, ignoring the terms containing the vev or the charged scalars. The same procedure can be done for the other fermions in a straightforward way.

$$\mathcal{L}_y^D = \overline{D}_L \kappa^D \tilde{h}_1 D_R + \overline{D}_L \rho^D \left(\tilde{h}_2 + i\tilde{h}_3 \right) D_R + h.c. \tag{29}$$

Now we substitute $\tilde{h}_i = h_j \tilde{R}_{ij}$, and rearrange a bit in order to arrive at

$$\mathcal{L}_y^D = D_L y_i^D \kappa^D D_R h_i + h.c. \tag{30}$$

where we have introduced the couplings y_i^F, defined as

$$y_i^U = \tilde{R}_{i1} + \varsigma^U \left[\tilde{R}_{i2} - i\tilde{R}_{i3} \right] \tag{31}$$

$$y_i^{D,E} = \tilde{R}_{i1} + \varsigma^{D,E} \left[\tilde{R}_{i2} + i\tilde{R}_{i3} \right] \tag{32}$$

Wee have also introduced the matrix ς^F, such that $\rho^F = \varsigma^F \kappa^F$. The above y_i^F are the same as in [11].

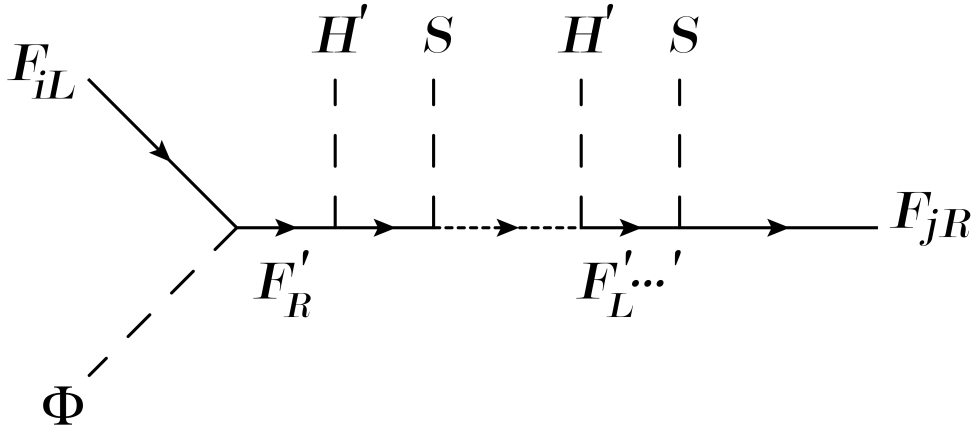

Figure 1: The sequence of BSM particles, F' etc, through which F_{iL} couples to F_{jR}.

3 Froggatt Nielsen Two Higgs Doublet Model

We shall now briefly discuss the Froggatt Nielsen mechanism, which is an attempt to explain the large differences in scale between the different fermion masses, as well as the magnitude of the elements in the CKM matrix. We also present the extension of this mechanism to the two Higgs doublet model. In the Froggatt Nielsen model, introduced in [3], we assume the existence of a new U(1) symmetry, and a corresponding conserved charge, which we shall refer to as the FN charge. We also assume the existence of a new scalar particle, S, with FN charge 1, no weak hypercharge, no color and that is an SU(2) singlet. This U(1) symmetry is then spontaneously broken, with S getting a non-zero vacuum expectation value [12]. We then assign different FN charges to the left handed doublets and to the right handed singlets for all standard model fermions, apart from the neutrinos. In contrast to the original model, [3], in the 2HDM version we also let the two Higgs doublets have different FN charges.

We consider a fermion of type $F \in \{U, D, E\}$, letting its corresponding doublet be denoted L^F. We assign to $F_{R,i}$ a charge $c - a_i^F$, where we let i be the generation. We assign a charge $c + b_j$ to L_j^F, again letting the subscript j denote the generation. We further assign to the Higgs doublets the charges R_n, $n = 1, 2$. Because of the conservation of FN charge, the Higgs fields can, generally, no longer couple directly between left and right handed particle states, but instead we must go through a number of intermediate states involving a number of heavy, BSM particles, F', F'', etc., see figure 1. Each intermediate particle gets mass from some unknown Higgs mechanism, involving a scalar, H', and switches chirality. It then couples to the next particle down the line, with an S carrying away one FN charge [12]. Assuming that all the Yukawa couplings are ~ 1, one finds that each intermediate step adds suppression by some factor, ϵ. The total number of steps required to go from F_i to L_j, via Φ_n, is $|a_i + b_j \pm R_n|$, where we have $+R_n$ for U, and $-R_n$ for D and E. The end

result is that we get an effective Yukawa lagrangian with effective Yukawa matrices

$$Y^F_{ij,n} \sim \epsilon^{|b^F_i + a^F_j \pm R_n|} \tag{33}$$

The hope is then, that by choosing these charge assignments properly, we can get the correct fermion masses, while also minimizing the FCNC's. It is still worth noting, however, that this only gives us the magnitude of the Yukawa couplings. The complex phases of the Yukawas are not given by the choice of charges, and we will consider them to be free parameters. The fact that this sets the off diagonal elements of the Yukawa matrices also makes it possible to derive the CKM matrix from the FN charge assignment.

In the above expression, ϵ is a real parameter, and is $\sim |V_{us}| \approx 0.2$, with V being the CKM matrix [13]. For a $\tan\beta = \epsilon^{-2} = 25$ the following charge assignments will yield the correct mass structure, and the correct CKM matrix, to leading order [14].

$$\begin{aligned} b^Q &= (3,2,0) & a^U &= (5,2,1) & a^D &= (2,1,1) \\ b^E &= (2,2,2) & a^E &= (5,2,-6) & R &= (-3,-1) \end{aligned} \tag{34}$$

To leading order, these charges give the following ρ matrices

$$\rho^U \sim \begin{pmatrix} \epsilon^5 & \epsilon^2 & \epsilon^1 \\ \epsilon^4 & \epsilon^1 & \epsilon^0 \\ \epsilon^2 & \epsilon^1 & \epsilon^2 \end{pmatrix} \tag{35}$$

$$\rho^D \sim \begin{pmatrix} \epsilon^8 & \epsilon^7 & \epsilon^7 \\ \epsilon^7 & \epsilon^6 & \epsilon^6 \\ \epsilon^5 & \epsilon^4 & \epsilon^4 \end{pmatrix} \tag{36}$$

$$\rho^E \sim \begin{pmatrix} \epsilon^{10} & \epsilon^7 & \epsilon^1 \\ \epsilon^{10} & \epsilon^7 & \epsilon^1 \\ \epsilon^{10} & \epsilon^7 & \epsilon^1 \end{pmatrix} \tag{37}$$

and the following κ matrices

$$\kappa^U \sim \begin{pmatrix} \epsilon^7 & 0 & 0 \\ 0 & \epsilon^3 & 0 \\ 0 & 0 & \epsilon^0 \end{pmatrix} \tag{38}$$

$$\kappa^D \sim \begin{pmatrix} \epsilon^6 & 0 & 0 \\ 0 & \epsilon^4 & 0 \\ 0 & 0 & \epsilon^2 \end{pmatrix} \tag{39}$$

$$\kappa^E \sim \begin{pmatrix} \epsilon^8 & 0 & 0 \\ 0 & \epsilon^5 & 0 \\ 0 & 0 & \epsilon^3 \end{pmatrix} \tag{40}$$

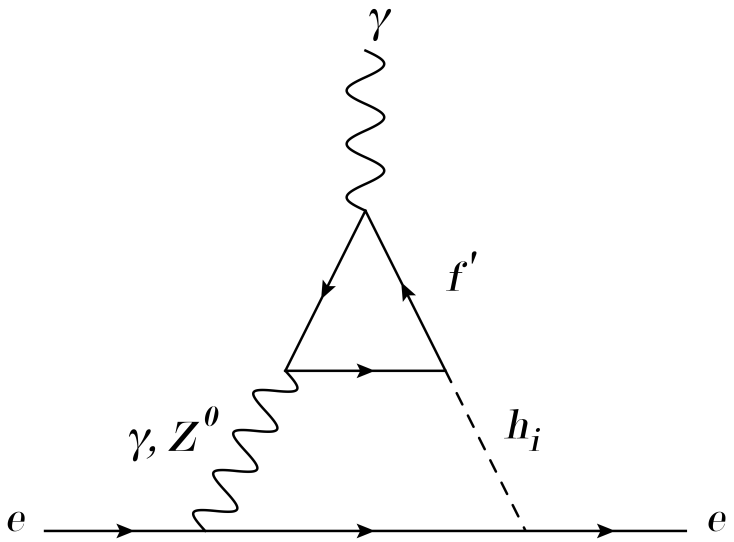

Figure 2: A Barr Zee diagram, contributing to the electron EDM.

4 Electron Electric Dipole Moment

We now turn towards the main focus of this study, namely the electric dipole moment of the electron. We will be looking at the contribution to the dipole moment from so called Barr Zee diagrams, specifically those in figure 2. Our approach follows closely that of [11].

The contribution to the electric dipole moment, from the diagram involving a top quark, is [9]

$$\left(\frac{d_e^\gamma}{e}\right)_t = \left[\frac{16}{3}\frac{\alpha}{(4\pi)^3}\sqrt{2}G_F m_e\right]\left\{\left[f\left(\frac{m_t^2}{m_{h_i}^2}\right)+g\left(\frac{m_t^2}{m_{h_i}^2}\right)\right]\mathrm{Im}Z_{0i}- \right. \\ \left. -\left[f\left(\frac{m_t^2}{m_{h_i}^2}\right)-g\left(\frac{m_t^2}{m_{h_i}^2}\right)\right]\mathrm{Im}\tilde{Z}_{0i}\right\} \quad (41)$$

with $Z_{0i} = y_i^f y_i^t$, and $Z_{0i} = y_i^f y_i^{t*}$ [11]. Extending this to also include other fermions than the top quark in the loop, and writing in terms of the couplings $y_i^f = (y_i^F)_{ff}$, the dipole moment is given, as in [11], by

$$\frac{d_e^\gamma}{2} = -2\frac{\sqrt{2}G_F\alpha}{(4\pi)^3}m_e q_e \sum_{f'}\sum_i q_{f'}^2 N_C^{f'}\left\{f\left(\frac{m_{f'}^2}{m_{h_i}^2}\right)\left(2\mathrm{Re}y_i^e\mathrm{Im}y_i^{f'}\right)+ \right. \\ \left. +g\left(\frac{m_{f'}^2}{m_{h_i}^2}\right)\left(2\mathrm{Im}y_i^e\mathrm{Re}y_i^{f'}\right)\right\} \quad (42)$$

Here, f' is used to denote the looping fermion. We use q_f, m_f and N_C^f to denote the charge, mass and number of color states respectively, of fermion f. The functions $f(z)$ and $g(z)$

are loop integrals given in [11] and [9]. For $z = 1$ we have that $f(z) \sim 1/2$ and $g(z) \sim 1$, and they behave such that for large z they are roughly logarithmic, whereas for small z they are both $\sim (z/2)(\ln z)^2$ [9].

We also include the contribution from the Z^0 in figure 2, given by

$$d_e^{Z^0} = -2\frac{\sqrt{2}G_F g_{Z\bar{e}e}}{64\pi^4} m_e q_e e \sum_{f'} \sum_i g_{Z\overline{f}f'} N_C^{f'} \left\{ \overline{f}\left(\frac{m_{f'}^2}{m_{h_i}^2}, \frac{m_{f'}^2}{M_Z^2}\right) \left(2\mathrm{Re}y_i^e \mathrm{Im}y_i^{f'}\right) + \right.$$
$$\left. + \overline{g}\left(\frac{m_{f'}^2}{m_{h_i}^2}, \frac{m_{f'}^2}{M_Z^2}\right) \left(2\mathrm{Im}y_i^e \mathrm{Re}y_i^{f'}\right) \right\} \quad (43)$$

with $g_{Z\overline{f}f} = g_W(T_3^f - 2q^f \sin^2\theta_W)/(2\cos\theta_W)$, where g_W is the weak coupling and T_3^f is the third isospin component of f. The loop functions $\overline{f}(x,y)$, and $\overline{g}(x,y)$ are as in [10], with

$$\overline{f}(x,y) = \frac{yf(x)}{y-x} + \frac{xf(y)}{x-y} \quad (44)$$

$$\overline{g}(x,y) = \frac{yg(x)}{y-x} + \frac{xg(y)}{x-y} \quad (45)$$

Since the looping fermion, and the electron, does not change flavor, we only include the diagonal couplings, $y_i^f = (y_i^F)_{ff}$. Since κ^F is diagonal, we have that $\varsigma^f = \rho^f/\kappa^f$, where we define $\kappa^f = (\kappa^F)_{ff}$ and $\rho^f = (\rho^F)_{ff}$, i.e. the diagonal element corresponding to f. The complex phase of ς^f is the same as that of ρ^f, which we will denote θ^f. We can then get the real and imaginary parts of y_i^f in terms of κ^f, $|\rho^f|$ and $\theta^f = \arg(\rho^f)$.

$$\mathrm{Re}(y_i^f) = \tilde{R}_{i1} + \frac{|\rho^f|}{\kappa^f}\left(\cos\theta^f \tilde{R}_{i2} - \sin\theta^f \tilde{R}_{i3}\right) \qquad f \in U \quad (46)$$

$$\mathrm{Re}(y_i^f) = \tilde{R}_{i1} + \frac{|\rho^f|}{\kappa^f}\left(\cos\theta^f \tilde{R}_{i2} + \sin\theta^f \tilde{R}_{i3}\right) \qquad f \in D, E \quad (47)$$

$$\mathrm{Im}(y_i^f) = \frac{|\rho^f|}{\kappa^f}\left(\sin\theta^f \tilde{R}_{i2} - \cos\theta^f \tilde{R}_{i3}\right) \qquad f \in U \quad (48)$$

$$\mathrm{Im}(y_i^f) = \frac{|\rho^f|}{\kappa^f}\left(\sin\theta^f \tilde{R}_{i2} + \cos\theta^f \tilde{R}_{i3}\right) \qquad f \in D, E \quad (49)$$

We will only be considering contributions where the looping fermion is either a top or a bottom quark.

Measurements of the electron electric dipole moment, or rather the lack thereof, put constraints on the magnitude of d_e. We will use the following value, from the ACME collaboration, as the upper limit [15]

$$|d_e| < 8.7 \cdot 10^{-29}\, e\,\mathrm{cm} \quad (50)$$

or in natural units

$$|d_e| < 1.4 \cdot 10^{-15}\,\mathrm{GeV}^{-1} \quad (51)$$

5 2HDMC

For the calculation of the electron electric dipole moment we have used the two Higgs doublet model calculator, 2HDMC [16]. 2HDMC is a program library for C++ that allows for various calculations in two Higgs doublet models, but the standard program assumes that CP is conserved in the scalar sector, and thus does not allow for an electron electric dipole moment. For this reason we have used a modified version from [5], which allows for calculations in a much more general model, as well as implementing a calculation of the eEDM. This version has, however, been further modified in order to allow for non-symmetric Yukawa matrices. The method for calculating the eEDM has also been modified so that it uses our expression, (42), for the eEDM, as well as allowing for complex Yukawa matrices in the eEDM calculation.

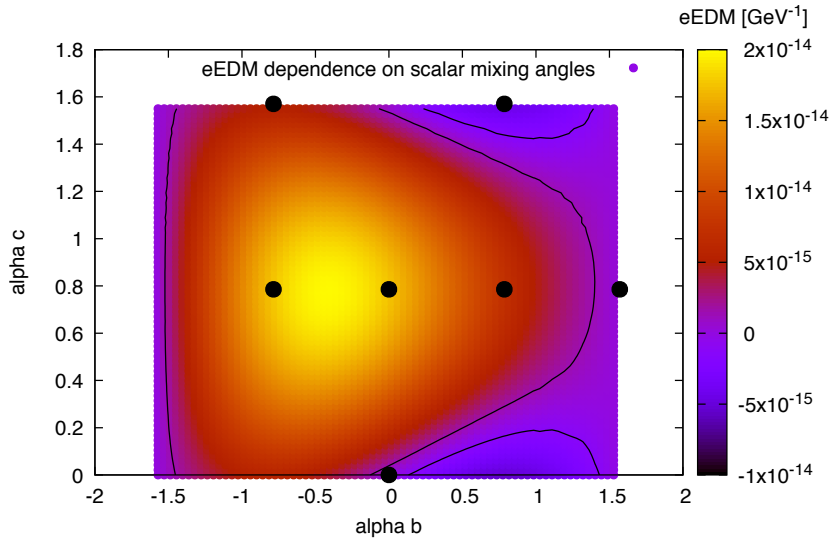

Figure 3: The dependence of the electric dipole moment, on the scalar mixing angles α_b and α_c. The hue shows the value of the dipole moment. The complex phases of the Yukawas are all set to 0. The neutral scalar masses are, $m_{h1} = 125$, $m_{h2} = 350$, $m_{h3} = 400$, all in GeV. The black dots indicate the points in the $\alpha_b - \alpha_c$ plane where we have later examined the θ^f, and m_{hi} dependence. The allowed regions are the small areas between the black lines.

6 Calculation of the Electric Dipole Moment

In this section we will study how the dipole moment changes as we vary the model parameters. In the first subsection we investigate how the dipole moment changes with α_b and α_c, as well as how it depends on the complex phases of the Yukawas. In the second subsection we study how the dipole moment depends on the masses of the neutral scalars. The results of our calculations are presented in the form of color maps, where the color of a point in the parameter plane corresponds to the value of the dipole moment at that point.

6.1 eEDM dependence on mixing angles and complex phases of the Yukawas

For all our calculations we work in the phenomenological basis used in [5]. In this basis, the free parameters are the scalar masses, the complex phases of the Yukawas, $\tan\beta$, $\cos(\beta-\alpha)$, α_b, α_c, $\mathrm{Re}\lambda_7$, λ_6 and $\nu = \mathrm{Re}(m_{12}^2)/(2v_1v_2)$. We set the scalar Higgs masses to $m_{h1} = 125\,\mathrm{GeV}$, $m_{h2} = 350\,\mathrm{GeV}$, $m_{h3} = 400\,\mathrm{GeV}$, and $m_{H^+} = 500\,\mathrm{GeV}$. We set $\tan\beta = 25$, and $\cos(\beta-\alpha) = 0$. We set $\nu = 2$, $\mathrm{Re}\lambda_7 = 0$, and $\lambda_6 = 0$. The magnitude of the Yukawa matrices are set according to (35-37).

Figure 3 shows how the electric dipole moment varies with different α_b and α_c, with all $\theta^f = 0$. We can see that most of the $\alpha_b - \alpha_c$ plane is forbidden, but there are regions that are viable. For $\alpha_b = \pm\pi/2$, the dipole moment will be in the allowed range. Similarly so for a small region surrounding $(\alpha_b, \alpha_c) = (0, 0)$ and $0, \pi/2$. There is also a narrow region connecting these two points and the right part of the diagram, which is allowed, for instance at $\alpha_b = \pi/4$, $\alpha_c \sim \pi/8$. We have marked a number of points in the $\alpha_b - \alpha_c$ plane, where we have chosen to investigate the dependence on the phases, θ^e, θ^t and θ^b, as well as the masses, m_{h2} and m_{h3}.

In figure 4, we have looked at the dependence on the Yukawa phases, for $\alpha_b = \alpha_c = 0$. We can see that the dependence on θ_t is heavily suppressed. This is surprising considering that the quark masses comes into (42) through the loop functions, which are roughly linear in $m_f^2/m_{h_i}^2$. Looking at the y_i^f couplings (46-49), we see that the dependence on θ^f is proportional to $|\rho^f|/\kappa^f = |\rho^f|v/m^f$, but this ratio is roughly the same for the top and the bottom quark.

We can see that if the bottom quark Yukawa coupling is entirely real, $\theta^q = 0$, π, then we have allowed regions for when the electron Yukawa is approximately real, $\theta^e \approx 0$, π. If we let the bottom quark Yukawa coupling be real, then we will have bands in the $\theta^e - \theta^b$ plane, that seem to approximately correspond to constant $\theta^e + \theta^b$, but with some periodic deviation from such lines.

The behavior of there being very little dependence on θ^t, compared to θ^b and θ^e, was the same for most choices of mixing angles, the one notable exception being for $\alpha_b = \pi/2$, and $\alpha_c = \pi/4$, see figure 5. We see that for this set of mixing angles, the dependence on θ^e is also somewhat suppressed, and for $\theta^b = 0$, it is comparable to θ^t. Looking at figure 5b, we see that for $\theta^b = 0$, there is barely any variation in the dipole moment with θ^e, which explains the behavior seen in figure 5a.

We see that all regions of 5a are allowed, since the dependence on $\theta^{e,t}$ is not large enough to give an EDM outside of the allowed range. In 5b, on the other hand, we have that $\theta^b = 0, 2\pi$ is allowed. We also have a band of allowed phases covering points such as, $(\theta^e, \theta^t) \sim (0, \pi)$, $(\pi/2, 3\pi/2)$, (π, π), and $(3\pi/2, \pi/2)$.

In figure 6 we have examined the dependence on θ^e and θ^t for the same parameters, but with $\theta^b = \pi$. We see in figure 5b that for this value of θ^b, we should have a strong dependence on θ^e, and indeed this is what we observe. This figure is similar to 4a, but with greater variation in the EDM. The allowed regions, again, consists of the bands $\theta^e = 0$, and $\pi/2$. The Higgs mixing matrix for this particular set of mixing angles is

$$\tilde{R} = \begin{pmatrix} 0 & 0 & 1 \\ \frac{1}{\sqrt{2}} & \frac{1}{\sqrt{2}} & 0 \\ -\frac{1}{\sqrt{2}} & \frac{1}{\sqrt{2}} & 0 \end{pmatrix} \tag{52}$$

We see that for these angles, $\tilde{h}_3 = h_1$, and the other two mass states will contain no CP-odd part.

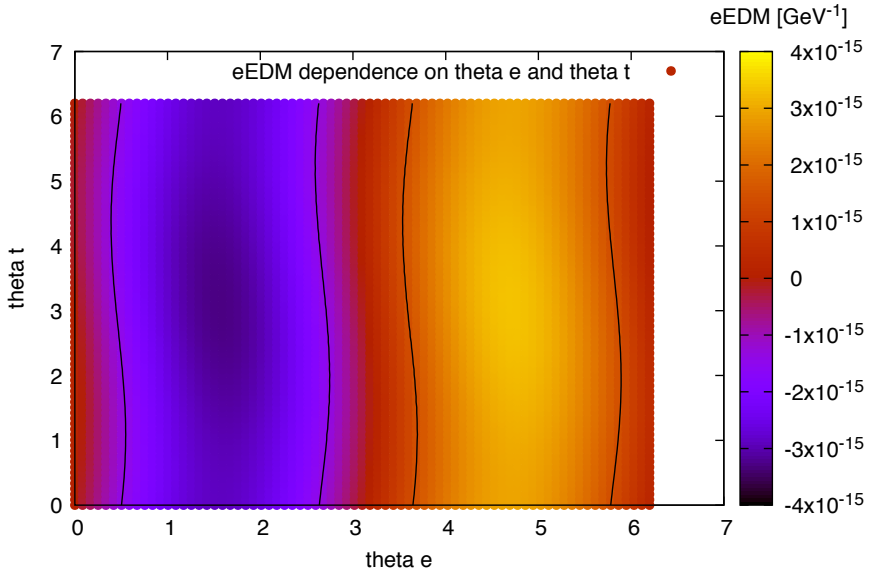

(a)

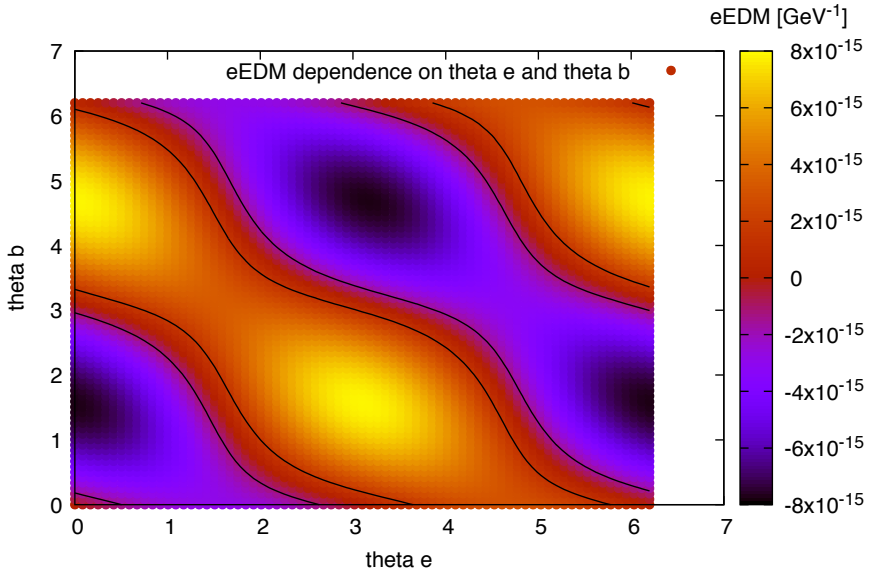

(b)

Figure 4: Dependence of the electric dipole moment on the complex phases of the Yukawas, θ^f. 4a shows the dependence on θ^e and θ^t, with $\theta^b = 0$. 4b shows the dependence on θ^e and θ^b, with $\theta^t = 0$. Mixing angles are $\alpha_b = \alpha_c = 0$. Masses are $m_{h2} = 350\,\text{GeV}$, $m_{h3} = 400\,\text{GeV}$. The allowed regions are the small areas between the black lines.

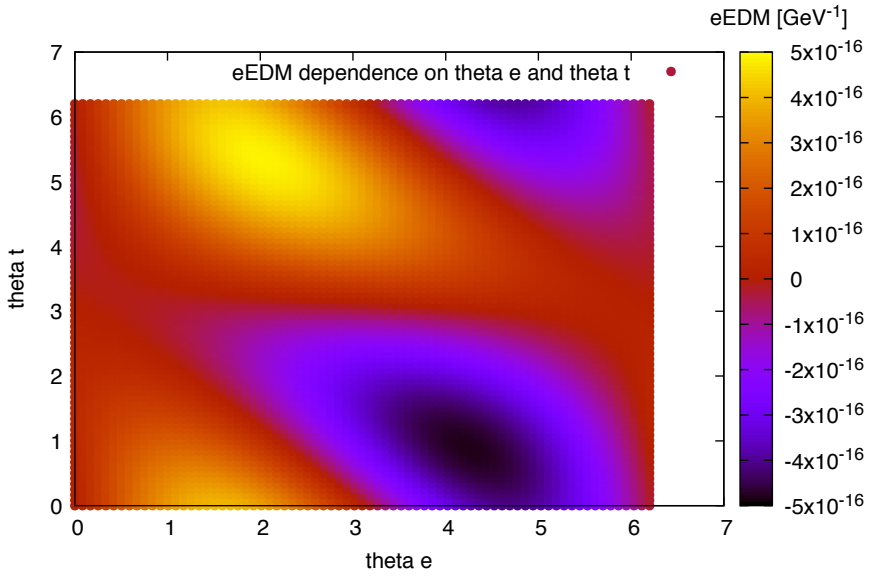

(a)

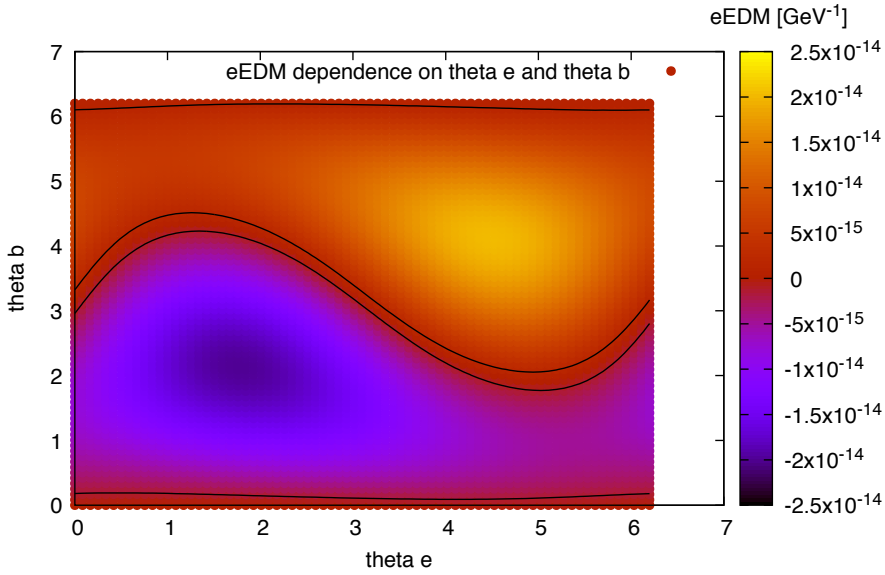

(b)

Figure 5: Same as figure 4, but with mixing angles $\alpha_b = \pi/2$, and $\alpha_c = \pi/4$. In (b), the allowed regions are the small areas between the black lines.

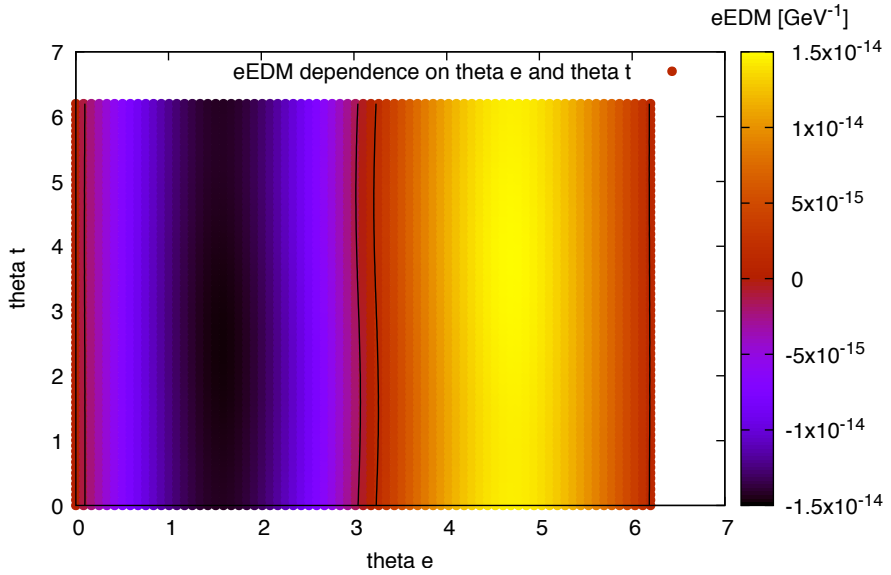

Figure 6: Same as figure 5a, but for $\theta^b = \pi$. The allowed regions are the small areas between the black lines.

In figure 7 we have varied the complex phases for $\alpha_b = -\pi/4$, $\alpha_c = \pi/4$. This corresponds to a region of the $\alpha_b - \alpha_c$ plane where we have a large contribution from scalar mixing. We see that even though the scalar mixing gives a relatively large contribution to the dipole moment, this can be canceled out by the CP-violation in the Yukawa sector. We can see that there is, again, very little dependence on θ^t. For $\theta^b = 0$ we have allowed regions in the form of two bands at $\theta^e \approx 3$ and $\theta^e \approx 4.5$. When we turn on θ^b, then we will find an allowed band at $\theta^b \approx 2.3$. We will find another band covering points $(\theta^e, \theta^b) \approx (2.7, 0)$, $(4.9, 0)$, $(1.2, 4.5)$ etc.

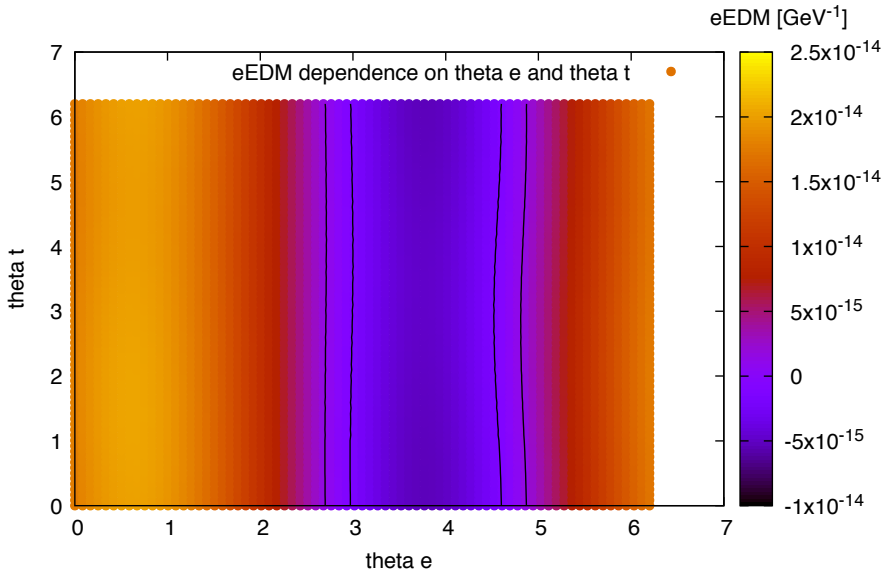

(a)

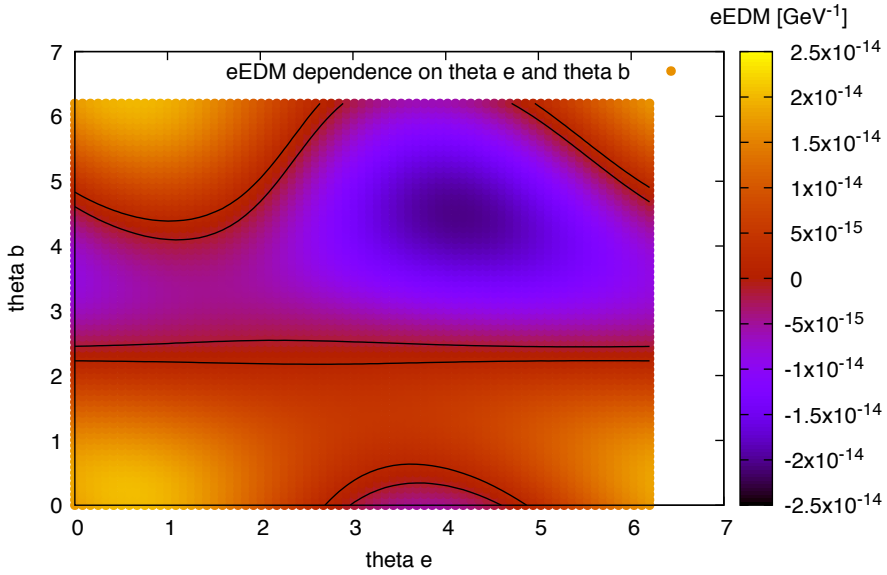

(b)

Figure 7: Same as figure 4, but with mixing angles $\alpha_b = -\pi/4$, and $\alpha_c = \pi/4$. The allowed regions are the small areas between the black lines.

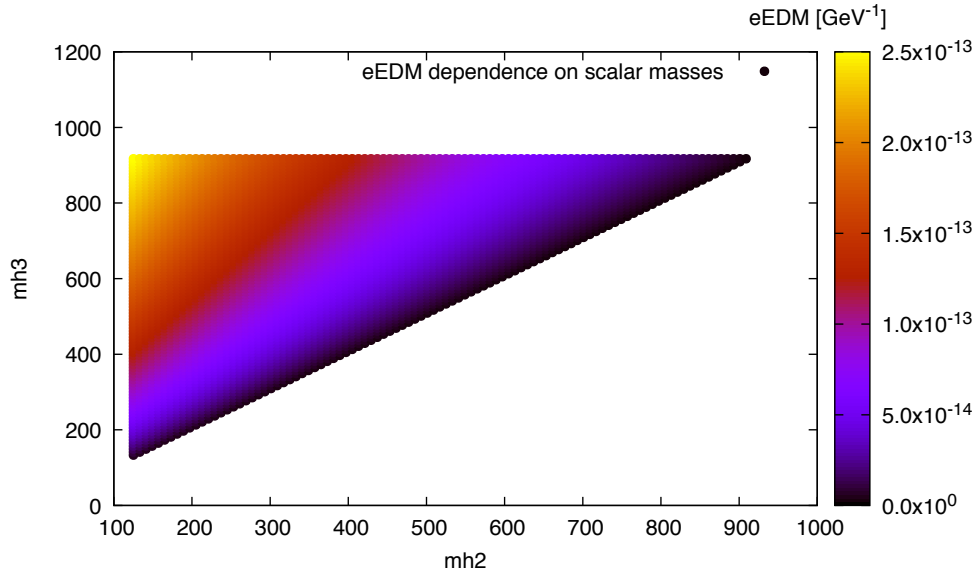

Figure 8: The dependence of the eEDM on the scalar masses, h_2 and h_3, for $\theta^f = 0$. The mixing angles are, $\alpha_b = 0$, and $\alpha_c = \pi/4$.

6.2 Dependence on the neutral Higgs masses

We now study the dependence of the dipole moment on the masses m_{h2} and m_{h3}. By definition, $m_{h2} \leq m_{h3}$. m_{h1} is still taken to be 125 GeV. We keep the other parameters the same as in the previous subsection, and set $\theta^f = 0$, for all fermions. We also point out that with $\sin(\beta - \alpha) = 1$, the quark mixing matrix reduces to

$$\begin{pmatrix} 0 & -\cos\alpha_b & \sin\alpha_b \\ \cos\alpha_c & \sin\alpha_b \sin\alpha_c & \cos\alpha_b \sin\alpha_c \\ -\sin\alpha_c & \sin\alpha_b \cos\alpha_c & \cos\alpha_b \cos\alpha_c \end{pmatrix} \tag{53}$$

Figures 8 and 9 shows the dependence on the Higgs masses for $\alpha_c = \pi/4$, and $\alpha_b = \pm\pi/4$, 0. We see that the dipole moment vanishes, as the two doublets get equal mass. For $\alpha_b = \pm\pi/4$ there is a, seemingly, small deviation from this, but for $\alpha_b = 0$ this cancellation seems to be exact. For $\alpha_b = 0$ and $\alpha_c = \pi/4$, the mixing matrix becomes

$$\tilde{R} = \begin{pmatrix} 0 & -1 & 0 \\ \frac{1}{\sqrt{2}} & 0 & \frac{1}{\sqrt{2}} \\ -\frac{1}{\sqrt{2}} & 0 & \frac{1}{\sqrt{2}} \end{pmatrix} \tag{54}$$

This means that h_1 will be the entirely CP-even, while h_2, h_3 will contain equal parts of the CP-odd state. Thus we get that in the limit of $m_{h2} = m_{h3}$, the eEDM will cancel.

For all three cases, almost all points are forbidden. Only for when the masses are very close to each other, almost exactly the same, are we within the allowed interval.

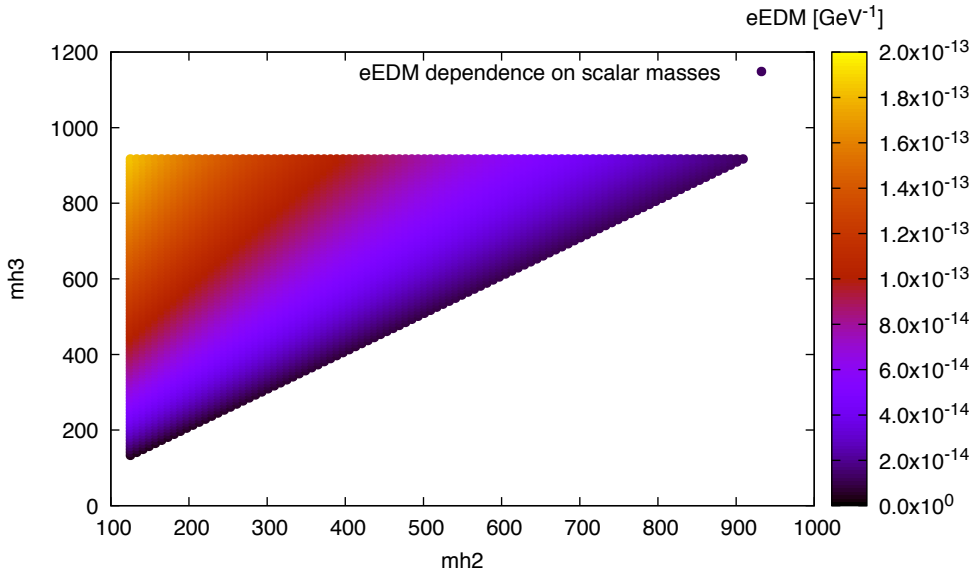

(a)

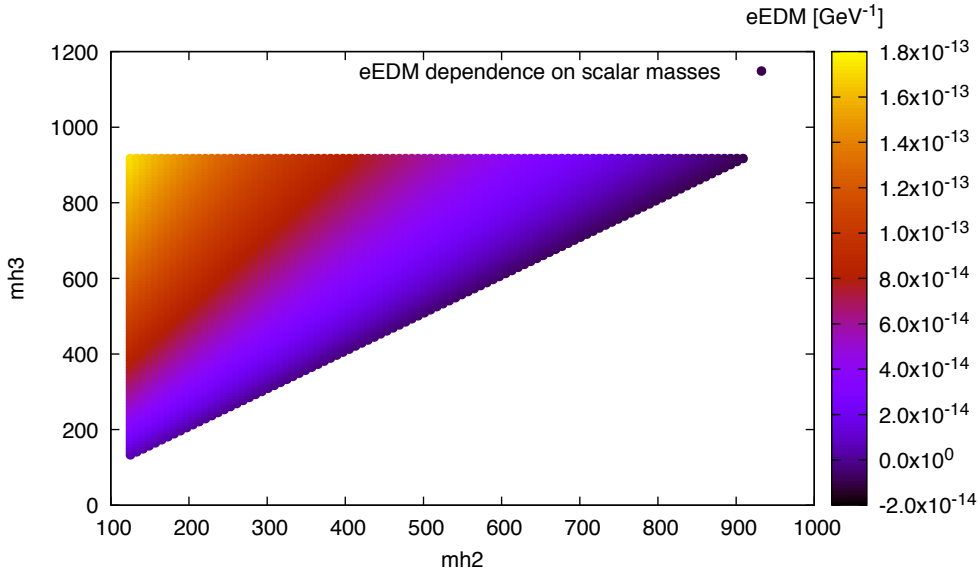

(b)

Figure 9: Same as 8, but for different Higgs mixing angles. 9a shows the mass dependence for $\alpha_b = -\pi/4$, $\alpha_c = \pi/4$. 9b shows the mass dependence for $\alpha_b = \pi/4$, $\alpha_c = \pi/4$.

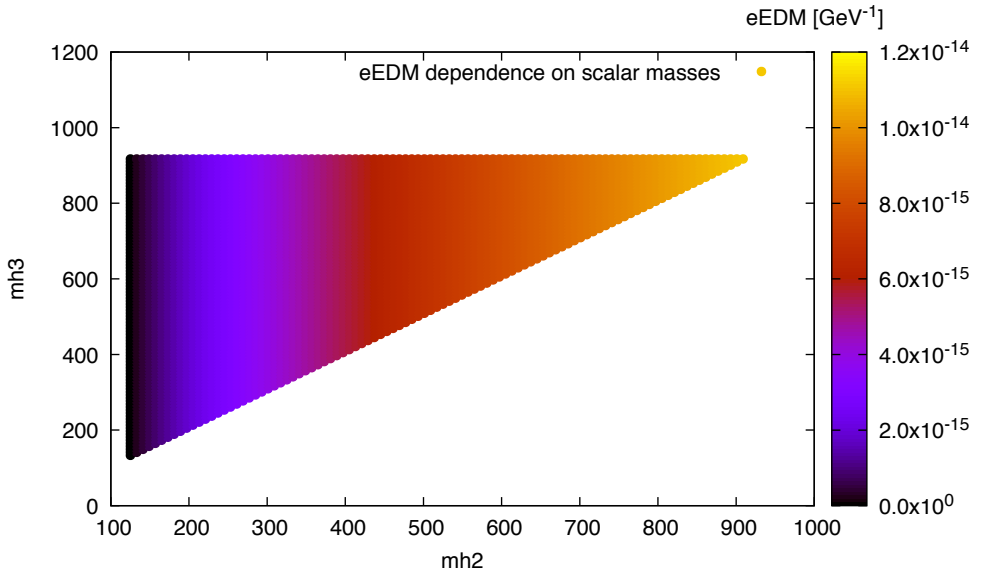

(a)

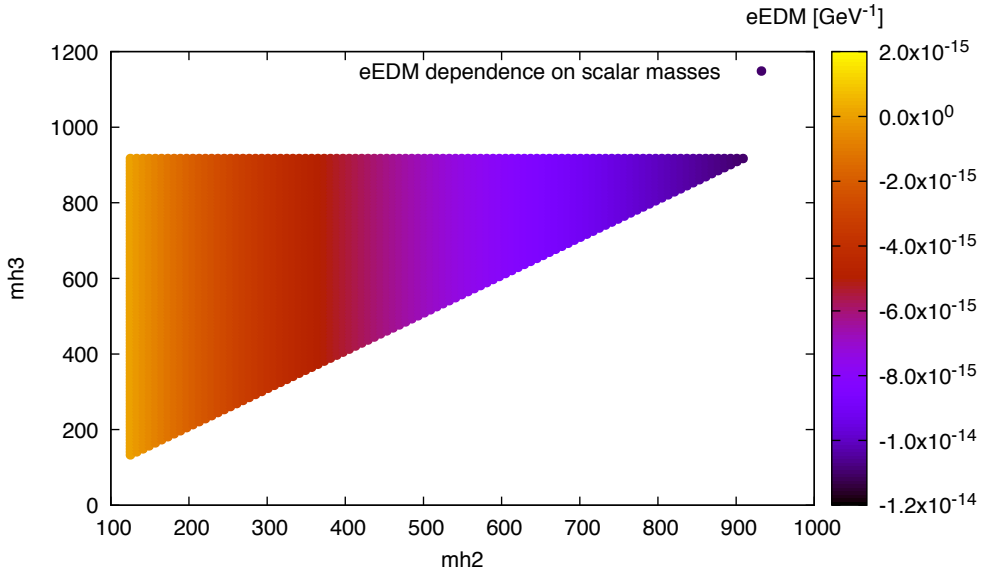

(b)

Figure 10: Same as 9, but for $\alpha_c = \pi/2$. 10a shows the mass dependence for $\alpha_b = -\pi/4$. 10b shows the mass dependence for $\alpha_b = \pi/4$.

Figure 10 shows the mass dependence for $\alpha_b = \pm\pi/4$ and $\alpha_c = \pi/2$. We see that there is barely any dependence on m_{h3} now, but that there is dependence on m_{h2}. We also notice that for $\alpha_b = -\pi/4$ the contribution is positive, whereas for $\alpha_c = \pi/4$ this contribution is negative.

Again we look at the mixing matrix. In this case it takes the form

$$\tilde{R} = \begin{pmatrix} 0 & -\cos\alpha_b & \sin\alpha_b \\ 0 & \sin\alpha_b & \cos\alpha_b \\ -1 & 0 & 0 \end{pmatrix} \tag{55}$$

We see that h_3 is now completely CP-even, explaining why the dipole moment does not depend on its mass.

In both diagrams we see that almost the entire region is forbidden, with only the very lowest values of m_{h2} being allowed. It seems that masses $\lesssim 220\,\text{GeV}$ are allowed, with no similar constraint on m_{h3}. We also see that in the limit, $m_{h1} = m_{h2}$, the contribution to the dipole moment vanishes.

7 Conclusions

We have examined the electric dipole moment of the electron in a Froggatt Nielsen 2HDM with CP violation in the Higgs and in the Yukawa sector. We have looked at how the dipole moment depends on the complex phases, θ^f, of the Yukawa couplings of the electron, and the top and bottom quarks. We have also looked at the dependence on the CP-violating Higgs mixing angles, α_b and α_c, as well as the masses of the neutral Higgs bosons, m_{h2} and m_{h3}.

In the case where there is no CP violation in the Yukawa sector, the CP-violating mixing angles are fairly constrained by the upper limit of the dipole moment. We found, however, that by adding CP-violation in the Yukawa sector, by letting θ^f be non-zero, it is possible to lower the dipole moment. This allows the mixing angles to potentially take on values that would otherwise be disallowed, although doing so might require a bit of fine tuning when both the top and bottom quark Yukawas have non-zero complex phases.

We found that, for some reason, the dependence on the top quark Yukawa phase is heavily suppressed. This is surprising, considering that the bottom quark contribution should be suppressed due to its low mass, compared to the top quark. We found no clear cause for this unexpected suppression of the top quark contribution.

When examining the dependence on the masses, m_{h2} and m_{h3}, we found interesting behavior where if we set α_c to $\pi/4$, the dipole moment decreases in the limit when $m_{h2} = m_{h3}$. There seemed to be, however, a small correction to this, for $\alpha_b \neq 0$. We found that this could be explained by the fact that for $\alpha_b = 0$, $\alpha_c = \pi/4$, the two scalars, h_2 and h_3, will contain equal parts of the CP-odd state, while h_1 will be entirely CP-even. Thus h_1 will provide no contribution, and in the limit of $m_{h2} = m_{h3}$, the contributions will cancel out.

If, on the other hand, α_c was set to $\pi/2$, then only m_{h2} seemingly affects the dipole moment. In this case the magnitude of the dipole moment increases with m_{h2}. Again the explanation came from the Higgs mixing matrix. For these mixing angles, only h_1 and h_2 will contain the CP-odd state, whereas h_3 will be CP-even, and thus, will not contribute.

In both the cases where we examined the mass dependence, we let the complex phases of the Yukawas be vanishing. Had these phases been non-zero, the above behavior would presumably be different.

In our calculations we have limited ourselves to one set of parameters, letting several of them be vanishing. The electric dipole moment is not the only constraint that can be put on our Higgs sector. The inclusion of additional constraints could mean that we are limited to a smaller subset of the $\alpha_b - \alpha_c$ plane, regardless of the Yukawa phases. We have also only looked at one particular set of FN charges, and it is quite possible that changing the charge assignments will affect the dipole moment, considering that this could change the ρ matrices. There are also further contributions to the dipole moment, other than the ones we have looked at. We have only considered the contribution of Barr-Zee

diagrams with a fermion loop, and the exchange of a neutral Higgs boson, but there will also be contributions from diagrams involving a charged Higgs and a $W^{\pm}$, as well as ones involving different fermions.

The biggest question that arose from our calculations is that of why the contribution to the EDM from the top quark was so suppressed. It is possible that this is the result of some bug in the code, either with the expression of the dipole moment itself, or possibly with the calculation of the loop integrals. When our code for calculating the EDM was checked against the one used in [5] for a case when both methods would work, i.e. with no CP-violation in the Yukawa sector, the results matched. The cause of this suppression should be investigated further.

References

[1] G. L. Kane, "Modern Elementary Particle Physics," 1992

[2] C. Patrignani *et al.* [Particle Data Group], Chin. Phys. C **40** (2016) no.10, 100001. doi:10.1088/1674-1137/40/10/100001

[3] C. D. Froggatt and H. B. Nielsen, Nucl. Phys. B **147** (1979) 277. doi:10.1016/0550-3213(79)90316-X

[4] G. C. Branco, P. M. Ferreira, L. Lavoura, M. N. Rebelo, M. Sher and J. P. Silva, Phys. Rept. **516** (2012) 1 doi:10.1016/j.physrep.2012.02.002 [arXiv:1106.0034 [hep-ph]].

[5] N. Hermansson Truedsson, (2016) http://lup.lub.lu.se/student-papers/record/8877188

[6] A. Dery and Y. Nir, JHEP **1704** (2017) 003 doi:10.1007/JHEP04(2017)003 [arXiv:1612.05219 [hep-ph]].

[7] J. Bijnens, J. Lu and J. Rathsman, JHEP **1205** (2012) 118 doi:10.1007/JHEP05(2012)118 [arXiv:1111.5760 [hep-ph]].

[8] S. Weinberg, Phys. Rev. Lett. **63** (1989) 2333. doi:10.1103/PhysRevLett.63.2333

[9] S. M. Barr and A. Zee, Phys. Rev. Lett. **65** (1990) 21 Erratum: [Phys. Rev. Lett. **65** (1990) 2920]. doi:10.1103/PhysRevLett.65.21

[10] S. Inoue, M. J. Ramsey-Musolf and Y. Zhang, Phys. Rev. D **89** (2014) no.11, 115023 doi:10.1103/PhysRevD.89.115023 [arXiv:1403.4257 [hep-ph]].

[11] M. Jung and A. Pich, JHEP **1404** (2014) 076 doi:10.1007/JHEP04(2014)076 [arXiv:1308.6283 [hep-ph]].

[12] J. Book, (2016) http://lup.lub.lu.se/student-papers/record/8887499

[13] M. Leurer, Y. Nir and N. Seiberg, Nucl. Phys. B **398** (1993) 319 doi:10.1016/0550-3213(93)90112-3 [hep-ph/9212278].

[14] E. Andersson, Personal Communication, To be published

[15] J. Baron *et al.* [ACME Collaboration], Science **343** (2014) 269 doi:10.1126/science.1248213 [arXiv:1310.7534 [physics.atom-ph]].

[16] D. Eriksson, J. Rathsman and O. Stal, Comput. Phys. Commun. **181** (2010) 189 doi:10.1016/j.CPc.2009.09.011 [arXiv:0902.0851 [hep-ph]].